Impact of Micropiles Installation on Liquefaction Potential of Saturated Silty Sand Using Numerical Method

Ehsan Taherabadi*, Seyed Abolhasan Naeini
Civil Engineering Department, Imam Khomeini International University, Qazvin, Iran.

Received: April 2017 Revised: Oct 2017

Abstract

This paper investigates the effect of micropile installation into saturated sandy soil by means of finite element method. The obtained results from numerical modeling are compared with the received data from the site. The validation of software has been done by simulating standard penetration test. The effect of some changes in spacing (3m, 1.6m and 0.8m) and injection pressure (1cm, 2.5cm, 5cm and 10cm boundary displacement) micropiles on liquefaction behavior was discussed. The results show that numerical modeling presented a conservative conclusion about the potential of liquefaction. The modification of soil increased by increasing injection pressure of grout. Also, it was observed that the effect of micropile spacing has less impact than the injection pressures up to 1m free distance of micropiles. Then for closer micropiles, the effect of spacing and the effect of pressure became bold and intensive, respectively. Because of direct relationship between number of SPT and liquefaction potential, it would be necessary to simulate SPT and

*Corresponding author e.taherabadi@edu.ikiu.ac.ir

[Downloaded from ndea10.khu.ac.ir on 2026-11-02]

[DOR: 20.1001.1.22286837.1398.13.5.2.1]

to validate with the real data, before and next of micropile installation. This approach can be a proper way of forecasting the efficiency degree of modification by micropiles and could save costs and time.

Keywords: Numerical simulation, micropile, saturated sand, liquefaction potential.

[Downloaded from ndea10.khu.ac.ir on 2026-11-02]

[DOR: 20.1001.1.22286837.1398.13.5.2.1]

Introduction

Micropile is a multipurpose system combined two kind of improvement (stabilization and reinforcement) together. This system is very effective in many applications of modification to increase the bearing capacity and decrease the settlement in retrofitting existing foundations and stabilizing slopes by supplying lateral strength.

Most of the researches paid attention to improvement bearing capacity and reduce settlement using micropiles (Bruce et al. [1, 2], Misra et al. [3, 4], Russo [5], Han and Ye [6] and Korolov and Argal [7] and Sharma et al. [8]). Sharma and Hussain [9], Veludo et al. [10], Galli and di Prisco [11] and Muthukkumaran [12] paid attention to static lateral bearing capacity of micropiles, numerically.

There is not a lot of experimental investigation about the dynamic behavior of micropiles and their connections (Shahrour [13], Shahrour and Sadek [14], Shahrour and Sadek [15], Alsaleh and Shahrour [16] and Ghorbani et al. [17]).

Among the numerical studies, it can be pointed to Babu et al. [18] who investigated static bearing capacity of inclined micropiles and

simulated plate load test (PLT) by using PLAXIS code. It is found that the bearing capacity increases up to 2 times by using micropiles corresponding to 25 mm settlement. McManus [19] studied the effect of vertical and inclined micropiles on the dynamic shear strain of sandy soil. He observed that the use of cross micropiles can decrease the cyclic shear strain up to half and soil settlement up to 20 percent of situation before micropile installation.

There is some literature about estimating the compression pressure or the amount of slush advance, provided by grouting. According to FHWA [20] maximum distance from the center of injection is between 125mm to 250mm that differ for every kinds of soils. These amounts are not the maximum amount of grout penetration. Teunissen [21] simulated a tunnel in 2D finite element program and exerted a radius pressure, as ordinary injection pressure used in nailing processes, perpendicular to the lining, and monitored the maximum total displacement around the tunnel to show the maximum radius of jointed rock, has been influenced by grouting. Hassanlourad [22] investigated sandy soils groutability by a kind of chemical grout made up of sodium silicate. Tests results showed that, particle size has the greatest effect on the grouting and the other mentioned parameters depend on this factor. In addition, for a pomp pressure of 1.2 MPa, water to sodium silicate ratio of 0.33, the maximum penetration of grout was obtained 19cm. This amount can be decrease by increasing in relative density. Ribeiro and Cardoso

[Downloaded from ndea10.khu.ac.ir on 2026-11-02]

[DOR: 20.1001.1.22286837.1398.13.5.2.1]

[23] collected all backgrounds of grouting in literature and declared their conclusions as three classified information as below:

1) For quality control of grouting, conceptual methods may be proper but it cannot predict the geometry of grouting before execution because the results of conceptual methods are from back analyses and are unique for each project.
2) Theoretical and semi-theoretical models reproduce injection operation but are not able to model how confinement pressure will be applied around grout mass. Also, the stress-state modification is vague in these methods.
3) SPH (smoothed particle hydrodynamics) method shows valid results by considering jet erosion and pressure transference to the soil. So, stress-state changes and all the deformations of model will be estimated.

Wang et al. [24] managed a numerical approach to estimate ground displacement due to horizontal grouting of undrained soft clay. The injection pressure was 30 MPa and the flow rate was 90 L/min. The results showed that by using Mohr-Columb constitutive model, the influencing radius is six times the radius of column. Shen et al. [25] assessed the lateral displacement due to jet grouting in clayey soils. An empirical equation that accounts for the jetting parameters (jetting pressure, flow rate of the fluid and rod withdrawal rate) and soil properties (soil type and its undrained shear strength) was developed to determine the radius of the plastic zone.

[Downloaded from ndea10.khu.ac.ir on 2026-11-02]

[DOR: 20.1001.1.22286837.1398.13.5.2.1]

Finally, for each type of sample (single borehole or group one) compared the existing approaches and presented a unique conclusion.

Some studies have been done using MATLAB code and artificial neural network to find a relation between the collected SPT data from liquefiable zones [26-29]. GuhaRay et al. [30] investigated the effects of micropiles of various diameters which had been placed at different spacing on reduction of liquefaction potential of sand experimentally. The results showed that spacing to diameter ratio of 6 to 7 is very effective in controlling liquefaction for a peak ground acceleration of 0.4 g using shake table.

Naeini and Hamidzadeh [31] studied the effects of the insertion of micropiles on prevention of liquefaction and improvement of subsidence through comparison of the results of Standard Penetration Test (SPT) and PLT before and after implementation of the micropiles. The results showed that SPT values and the ultimate bearing capacity of silty sand increased after installation of micropiles at 2.3 m distances.

As it mentioned, the past studies around micropiles and their effectiveness are so embellished that concentration on a single issue is sufficient for every researcher. Then, because of low investigation about estimating the effect of micropile installation on liquefiable soils by the index of standard penetration test, it seems to be necessary to combine the micropile installation issue and in situ test results.

[Downloaded from ndea10.khu.ac.ir on 2026-11-02]

[DOR: 20.1001.1.22286837.1398.13.5.2.1]

This research has been done to simulate standard penetration test, carried out by Ziaei and Naeini [32] in the low altitude strip of coastal land next to the Caspian Sea before. After verification, the impact of micropile presence in the saturated sandy soil has been modeled. In this paper, standard penetration test has been simulated at first, then presence of micropile in saturated silty sand and its effect on number of SPT has been investigated by using finite element software (PLAXIS, V.8.5). Results of modeling were compared with the site information (SPT data) and then the model was developed by some changes in micropiles distance and injection pressure.

Field study

Site Characterization

Naeini and Ziaei performed a development project and investigated the potential of liquefaction by SPT. They drilled 3 boreholes to identify soil layers by using rotary drilling machine up to 30m depth in specified location. The disturbed and undisturbed sample had been taken at every 2m depth for classification and determination of chemical and physical characteristics of soil [32]. The deposits of coast were made up of silty sand (SP-SM & SM). Some silty layers observed at some depths. It is estimated 0.85 and 0.50 as the average of maximum and minimum porosity. Finally, the soil layers were divided into two parts. First is a 20m layer consists of medium and second is 10m layer consists of very dense silty sand on the basis of SPT results. The soil specification has been showed in Table 1.

[Downloaded from ndea10.khu.ac.ir on 2026-11-02]

[DOR: 20.1001.1.22286837.1398.13.5.2.1]

Table 1. In situ mechanical specifications of soil layers before and after micropile installation [32]

USGS	Z (m)	σ_v (kPa)	$\acute{\sigma}_v$ (kPa)	CSR		$(N_1)_{60}$	CRR	F.S.	Φ (°)	γ (kN/m^3)	E (kN/m^2)	D_r (%)	e_0	Δe
ML	3.5	66.5	31.5	0.468	N	22	0.234	0.498	35	18	8000	60	0.64	0.07
					R	35	0.567	1.21	40	20	11000	80	0.57	
SM	12	228	108	0.411	N	18	0.189	0.461	34	18	7200	55	0.658	0.108
					R	39	1.01	2.456	41	21	13500	85	0.55	
	13.5	257	122	0.388	N	16	0.177	0.456	35	18.5	6600	50	0.675	0.077
					R	32	0.412	1.06	38	20	11000	72	0.598	
	15	285	135	0.365	N	12	0.129	0.355	33	17	5000	37	0.72	0.108
					R	33	0.46	1.258	41	17.5	11000	68	0.612	
	17	323	153	0.334	N	24	0.273	0.817	38	19	9000	57	0.65	0.045
					R	34	0.509	1.523	45	20	12000	70	0.605	

N: Natural and R: Reinforced

Micropile system was chosen as modification mechanism. The piles were drilled and grouted within 12.5 to 30.5 centimeter diameter with one bar (Φ28 or Φ25) as the reinforce element in the center of the hole to resist the bulk of design load. A reticular casing with 75mm and 68 mm as external diameter and internal diameter, respectively, also had been used. Two-step process of grout placement (Type C) had been used to micropile installation. At first, gravity grouting (Type A) had been performed and then after 15 minutes the secondary pressure grouting through sleeved pipe with 1.2 MPa pressure were carried out. 300 to 340 lit/meter grout had been used for each micropile installation. It was observed that the soil groutability should be up to 4.5 times of the theoretical value (excavated borehole volume). This fact is representative of the very porous nature of the beach deposits.

[Downloaded from ndea10.khu.ac.ir on 2026-11-02]

[DOR: 20.1001.1.22286837.1398.13.5.2.1]

Numerical modeling

Each impact SPT hammer changes the stress surface of the soil. In the other words, the mechanical specifications such as elasticity modulus, internal friction angle, cohesion, relative density and soil failure stress, should be replaced by new data. Some of these changes may be done by defining hardening soil (HS) model or softening soil (SS) model. However, having hardening curve of every soil layer could not be useful to simulate SPT as a numerical model. Nevertheless, in the absence of some detailed experimental data, it is feasible to run a model by using the ability of changing some parameter with depth or time or temperature.

There are two general ways to simulate numerically: 1) direct and, 2) indirect. In direct simulation, the model is built accurately and very similar to what happens in reality by accessing the required data for processing but in indirect simulation, there is an attempt to extract some close and rational results, in harmony with the actual results. So it is possible to apply some simplifications and trials to achieve the desire result.

In this paper, a modal analysis was developed to determine Rayleigh damping coefficients. Then, as a direct way, SPT has been modeled with minimum simplifications to attain number of SPT as an index of soil terms of compaction, before and after micropile installation. Instead of modeling the impacts of SPT hammer, the effect of micropile installation and jet grouting has been simulated as the indirect way. As grout injection procedure causes large

[Downloaded from ndea10.khu.ac.ir on 2026-11-02]

[DOR: 20.1001.1.22286837.1398.13.5.2.1]

deformation in soil, a Lagrangian approach, must be used to reach converged answers. Lagrangian analyses do not require to make the stiffness matrix. So, in large displacements every node updates at each time step and occurred displacements are added to the past coordinates of points. As the result, the elements supplanted and the geometry of model changes.

At first, Rayleigh damping coefficients have been extracted by modal analysis on finite element (FE) software (ABAQUS). For the purpose, every soil layer was modeled separately and was allowed to settle statically. Three phases were introduced to run the simulation. First phase was "soil" (for settlement of undrained soil block) and second phase was "static general" (for settlement of undrained soil block at presence of surcharge). Modal analyses were carried out by introducing third phase known "frequency" from linear perturbation subset. Outputs of the software were initial modes (f_1, f_2, f_3 and …) Noted that the used constitutive model was Mohr-Columb and all the layers set to be undrained. The coefficients should be calculated with relations (1) and (2).

$$\alpha = \xi_{\min} . \omega_{\min} \tag{1}$$

$$\beta = \xi_{\min} / \omega_{\min} \tag{2}$$

Where α and β are Rayleigh damping coefficients, ξ_{min} is about 0.05 and ω_{min} is minimum angular velocity (= $2\pi F_{min}$).

Second step is to set a model of SPT, as a regression analysis to find out α and β. Then it was made a comparison with the results of

[Downloaded from ndea10.khu.ac.ir on 2026-11-02]

[DOR: 20.1001.1.22286837.1398.13.5.2.1]

modal analysis. Providing the model has been done by following considerations:

1) Model dimensions were chosen by paying attention to the depth of test and stress penetration.
2) Because of small diameter of SPT sampler, circular area has been considered instead of ring cross section, representative the region of applied load. Figure 1 shows the deformed mesh of model after analysis at the depth of 13.5 m as a sample.

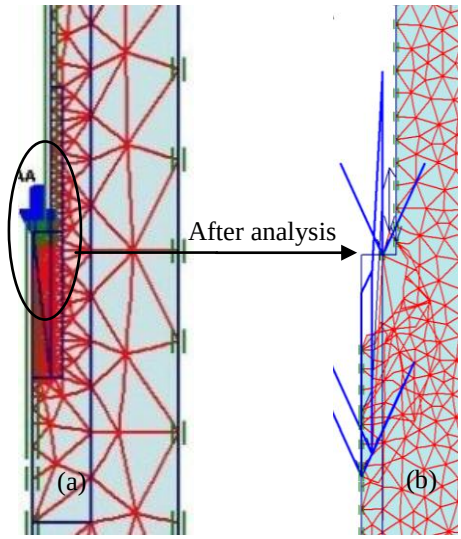


Figure 1. Mesh and geometry of model before analysis (a), deformed mesh under SPT hammer (b), at the depth of 13.5 m as a sample.

3) Axisymmetric method of modeling has been used to exert the effects of confinement in the absence or presence of micropiles.
4) Impact of hammer was modeled by considering momentum law (Figure 2).

[Downloaded from ndea10.khu.ac.ir on 2026-11-02]

[DOR: 20.1001.1.22286837.1398.13.5.2.1]

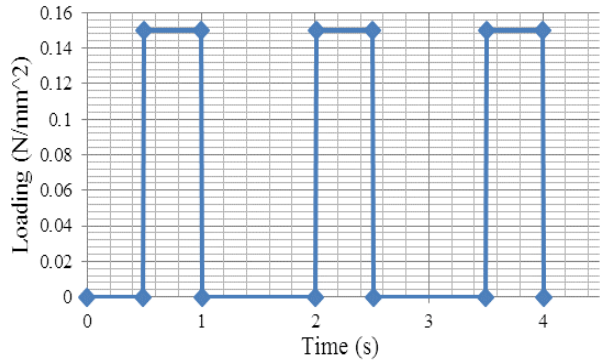


Figure 2. Loading curve

5) Triangular elements with 15 nodes were set to assign mesh. Around the critical zone of model (falling location of hammer) was chosen to refine mesh and increase the accuracy of model.

6) Boundary conditions were placed to form of absorbent boundary to avoid reflexing dynamic waves into the model due to impact loading.

7) Water table set to be on the surface ground. The undrained Mohr-Clolumb analyses were considered for all soil layers.

8) Micropile structure has not been modeled because stress contours due to falling SPT hammer cannot meet the affected areas by micropiles.

9) Soil specification and layers were set according to the base study (Table. 1). The Rayleigh damping coefficients for modal and regression analysis before micropile installation have been showed in Table 2.

[Downloaded from ndea10.khu.ac.ir on 2026-11-02]

[DOR: 20.1001.1.22286837.1398.13.5.2.1]

Table 2. Comparison of regression analysis and modal analysis in calculating Rayleigh coefficients.

Results of regression analysis						Results of modal analysis				
17	15	13.5	12	3.5	Depth (m)	3.5	12	13.5	15	17
0.417	0.357	0.625	0.384	0.5	α	0.4545	0.403	0.645	0.6	0.385
0.006	0.007	0.004	0.0065	0.005	β	0.0055	0.0062	0.00387	0.00417	0.0065

The attained coefficients had some differences with regression analysis. The error of this trial is lesser than 15%.

The next step is to model SPT with attained Rayleigh coefficients from modal analysis. Considerations were taken into account similar to step 2. The SPT N-value attained from the number of required phases representative to the number of falling SPT hammer to get 30 cm soil penetration. Figure 3 shows the comparison between PLAXIS and real results of $N_{(SPT)}$.

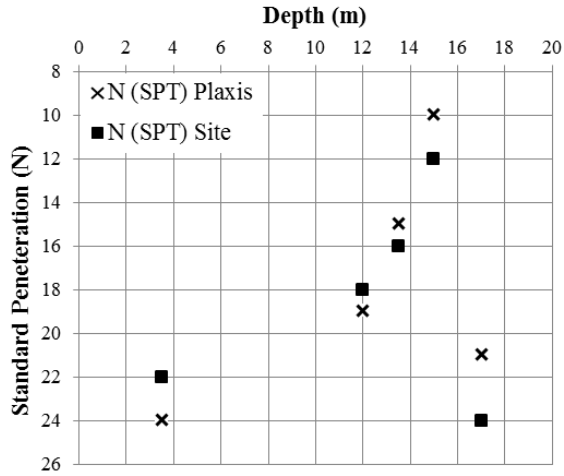


Figure 3. Comparison between PLAXIS and real results of $N_{(SPT)}$.

The maximum error of SPT N-value is 12.5% which occurs at higher depths and can be acceptable (Figure 3). However, the

[Downloaded from ndea10.khu.ac.ir on 2026-11-02]

[DOR: 20.1001.1.22286837.1398.13.5.2.1]

attained results from numerical simulation exhibited higher amount than in situ data at shallower depths, but there are adverse results by entering the liquefiable layer at higher depths.

In indirect method, at first a model simulated in axisymmetric method to create surrounded pressure, considering the effect of nearby micropiles. Model consists of 15 nodes of triangular elements arrange. The dimension of model was 20m height × 5m width. Validation of the model to in situ evidence was performed by establishment of site condition and 3m spacing of micropiles as implemented. The soil behavior was described using an elastoplastic constitutive model based on the non-associated Mohr-Columb criterion and the parameters were chosen according to Table 1. Proper boundary conditions were used to ensure the displacement transmission through the center boundary of soil mass. Water table sets on the surface of soil block. Changing the stress level by applying undrained condition, non-occurrence of tensile crack and gradient changes in elastic modulus are modeled approximately. In this paper the changes in injection pressure introduced as displacement to the model. Two steps were introduced to run the analyses. The first step produced the geostatic situation and the second exerted the displacement into the boundary after resetting the displacements of the first step to zero. Figure 4 shows a sample of applied horizontal displacements (1 cm) at 3 m spacing of micropiles.

[Downloaded from ndea10.khu.ac.ir on 2026-11-02]

[DOR: 20.1001.1.22286837.1398.13.5.2.1]

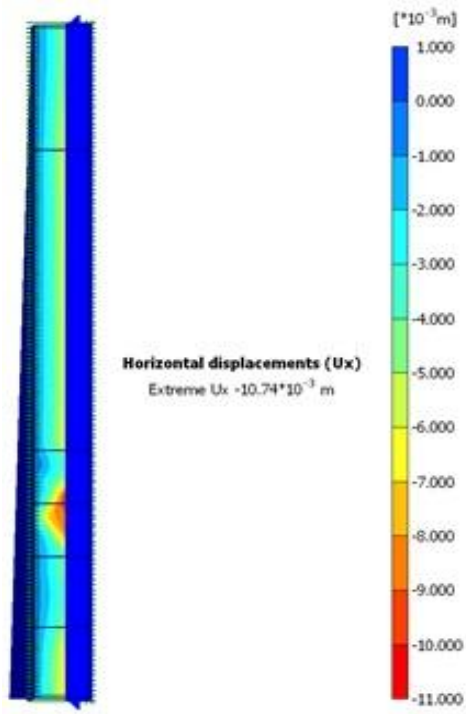


Figure 4. Changes of horizontal displacement of model due to applying horizontal displacements (1 cm) at 3 m spacing of micropiles.

For converting the results of displacement into some data such as N_{30}, the following procedure has been run:

1) A region, parallel to external boundary at 30mm distance of it, has been considered. The philosophy was to calculate the displacement of soil at the mentioned region and to determine porosity index by using relation (3):

$$\Delta H/H = \Delta e/1 + e0 \quad (3)$$

Where ΔH is horizontal displacement, H is distances between micropiles, Δe is changing in porosity and e_0 is initial porosity.

[Downloaded from ndea10.khu.ac.ir on 2026-11-02]

[DOR: 20.1001.1.22286837.1398.13.5.2.1]

2) Having ΔH could help attain relative density and consequently attain N_{30} as definition of Bowles according to Table 3 [33].

Table 3. Experimental values for SPT N-value, internal friction angle and density of soil block on the basis of the quality of compression [33].

Description		Very loose	Loose	Medium	Dense	Very dense
Relative density D_r		0	0.15	0.35	0.65	0.85
SPT N'_{70}:	fine	1–2	3–6	7–15	16–30	?
	medium	2–3	4–7	8–20	21–40	> 40
	coarse	3–6	5–9	10–25	26–45	> 45
ϕ:	fine	26–28	28–30	30–34	33–38	
	medium	27–28	30–32	32–36	36–42	< 50
	coarse	28–30	30–34	33–40	40–50	
γ_{wet}, kN/m^3		11–16*	14–18	17–20	17–22	20–23

3) In NCEER-97directive Seeds recommendations are used to assess the liquefaction potential in sandy soils. Two quantities have to be determined: 1) Cyclic Stress Ratio (CSR) and 2) Cyclic Resistance Ratio (CRR). Using Seed and Idriss (1981), CSR is determined using equation (4).

$$CSR = {}^{\tau_{av}}/_{\sigma'_{v0}} = 0.65\left({}^{a_{max}}/_{g}\right)\left({}^{\sigma_{v0}}/_{\sigma'_{v0}}\right) r_d \qquad (4)$$

Where a_{max}, g, r_d, σ'_{v0}, σ_{v0} and τ_{av} are maximum horizontal ground acceleration at ground surface in m/s^2 (equal to 0.35g), ground acceleration in m/s^2, shear reduction coefficient with depth, effective overburden pressure in kPa, total overburden pressure in kPa and average shear strength in kPa, respectively. The NCEER has recommended the relations (5) and (6) to determine shear stress reduction coefficient with depth (rd).

[Downloaded from ndea10.khu.ac.ir on 2026-11-02]

[DOR: 20.1001.1.22286837.1398.13.5.2.1]

$$r_d = 1.0 - 0.00765 \times Z \qquad Z < 9.15\ m \tag{5}$$

$$r_d = 1.174 - 0.0267 \times Z \qquad 9.15 < Z < 23\ m \tag{6}$$

Determination of CRR based on SPT results presented in Figure 5 which had been proposed by Seed et al. (1983).

4) The factor of safety against liquefaction is determined with relation (7).

$$FS = CRR/CSR \tag{7}$$

Figure 6 compares the results of safety factors of modeling and in

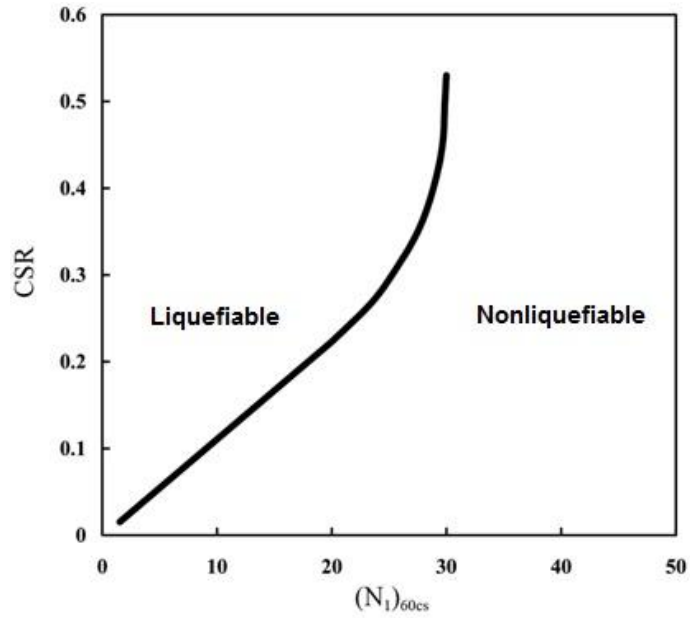


Figure 5. Cyclic Resistance Ratio (CRR) for Clean Sands Under Level Ground Condition Based on SPT (Recommended by Seed et al. 1983)

situ data for 3 meter of spacing of micropile, before micropile installation according to indirect method. As can be seen in Figure 6, there is small difference between site and model results. On the other words, at all depths except 17m, the harmony between in situ and

[Downloaded from ndea10.khu.ac.ir on 2026-11-02]

[DOR: 20.1001.1.22286837.1398.13.5.2.1]

model results can be observed. It might be due to the increasing rate of the relative density of soil layer, with increasing depth. This fact couldn't depict in the above layers because of low thickness of the layers which have identical and constant D_r in depth. So, it can be concluded that such a simple model like above one may persuade engineers to trust to the software in forecasting the liquefaction potential of silty sand after retrofitting by micropiles.

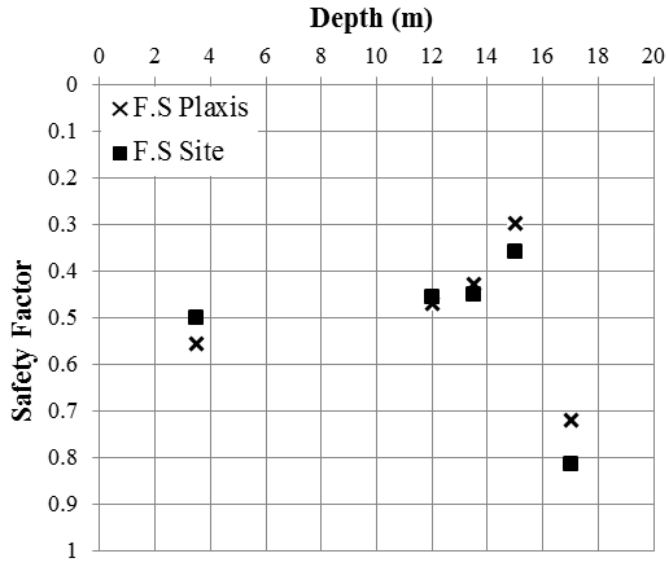


Figure 6. Safety factor before micropile installation for spacing 3m

Results

Model improvement has been done by presence of micropiles in some distances (3, 1.6 and 0.8 m) and by applying some changes in boundary displacement (1, 2.5, 5, and 10 cm), representative injection pressure. After simulation of micropile installation

[Downloaded from ndea10.khu.ac.ir on 2026-11-02]

[DOR: 20.1001.1.22286837.1398.13.5.2.1]

according to the mentioned procedure, the following results have achieved in the term of $N_{(SPT)}$. Figures7 to 9 show the comparison of N_{SPT} changes with depth, for four grouting intensity (boundary displacement) at micropiles distance of 3, 1.6 and 0.8 meter. It is not noticeable, the modification of 1cm boundary displacement at 3m distance of micropiles, because the stress bulb due to hammer impacts cannot be influenced by the boundary displacement.

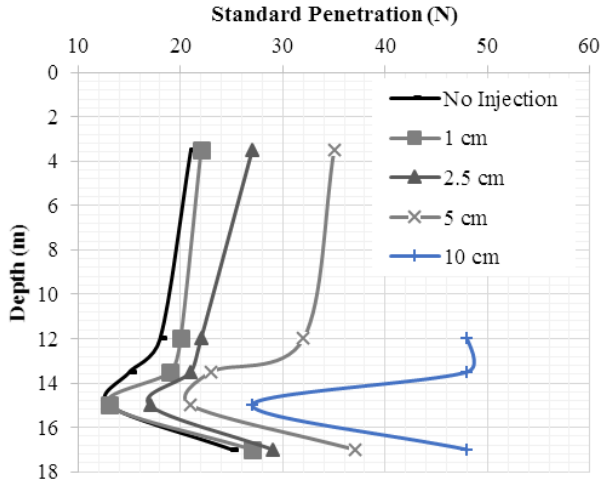


Figure7. Comparison of N_{SPT} changes with depth at micropiles distance of 3 meter.

By increasing injection pressure, layer modification and the rate of modification increase. Maximum improvement of liquefiable layer attains from injection pressure equal to 5cm of boundary displacement at 1.6m distance of micropiles. Saturate condition reduces the efficiency of grouting and demands more pressures for improvement. There are some eliminated data at boundary displacements because of exceeding the limit of 50 impacts as the

[Downloaded from ndea10.khu.ac.ir on 2026-11-02]

[DOR: 20.1001.1.22286837.1398.13.5.2.1]

number of standard penetration test. It means that the soil layer would be safe and dense enough to prevent liquefaction.

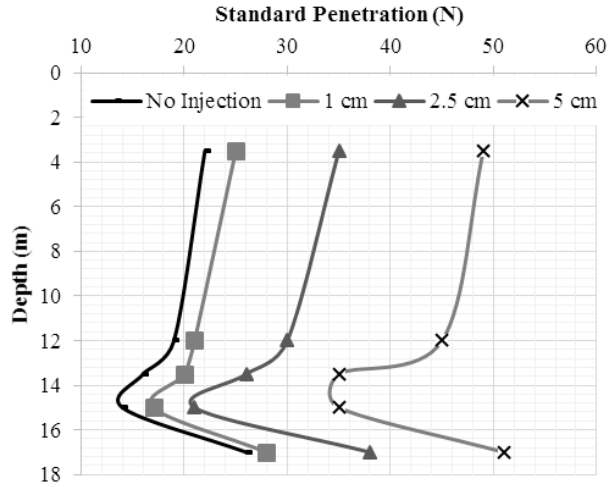


Figure 8. Comparison of N_{SPT} changes with depth at micropiles distance of 1.6 meter.

Another comparison has been made for investigating the effect of modification at the same depth by various boundary displacements. Figures 10 to 14 show the comparison of N_{SPT} changes with boundary displacement at the depth of 3.5, 12, 13.5, 15 and 17m, respectively.

As can be seen in Figures 10 to 14, the rates of modification are

[Downloaded from ndea10.khu.ac.ir on 2026-11-02]

[DOR: 20.1001.1.22286837.1398.13.5.2.1]

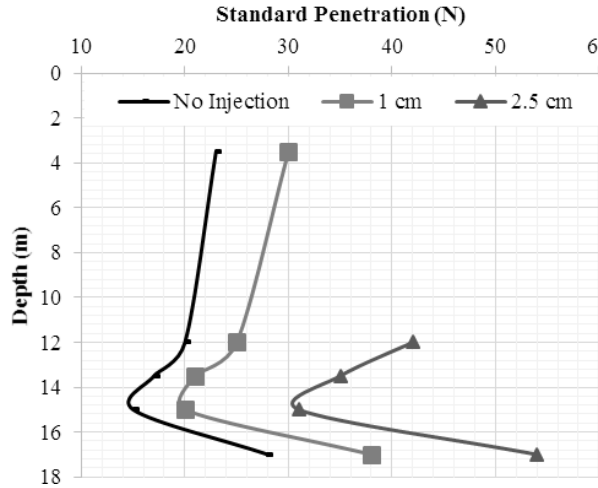


Figure 9. Comparison of N_{SPT} changes with depth at micropiles distance of 0.8 meter.

higher at the closer distances of micropiles and it would be adequate to use less injection pressure for success. Also, it is obvious to recognize nonlinearity of the results of $N_{(SPT)}$ with the boundary displacements. That is by increasing the boundary displacement at the constant rate, the $N_{(SPT)}$ increases non-fixed rate. It is clear that the achieved modification occurs at the closer free distance of micropiles, at the same injection pressure.

Table 4 summarizes the achieved results about liquefaction potential of sandy soil, reinforced by micropiles. As can be seen, the true injection pressure to control liquefaction potential at 0.8m, 1.6m and 3m distance of micropiles are 2.5, 5 and 10 cm respectively. On the other hand, some layers may fail by high injection pressure. For example, there is a liquefiable soil ($N_{SPT} < 30$) at 3m spacing of micropiles but at 10 cm boundary displacement it is expected to fail

[Downloaded from ndea10.khu.ac.ir on 2026-11-02]

[DOR: 20.1001.1.22286837.1398.13.5.2.1]

nonliquefiable layers (Figure 7).

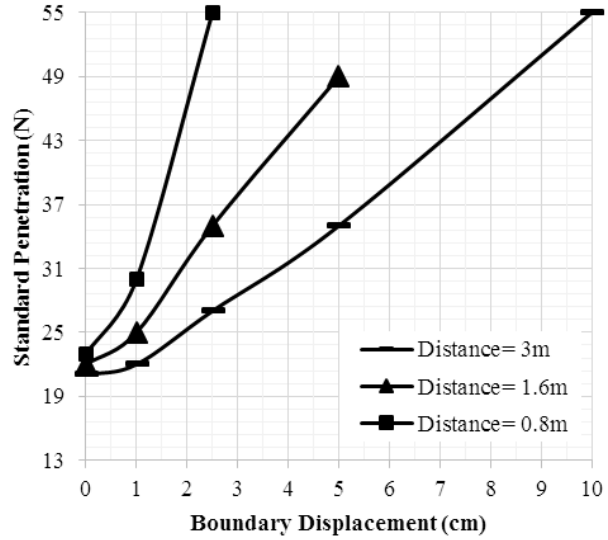


Figure 10. Comparison of N_{SPT} changes with boundary displacement at the depth of 3.5m.

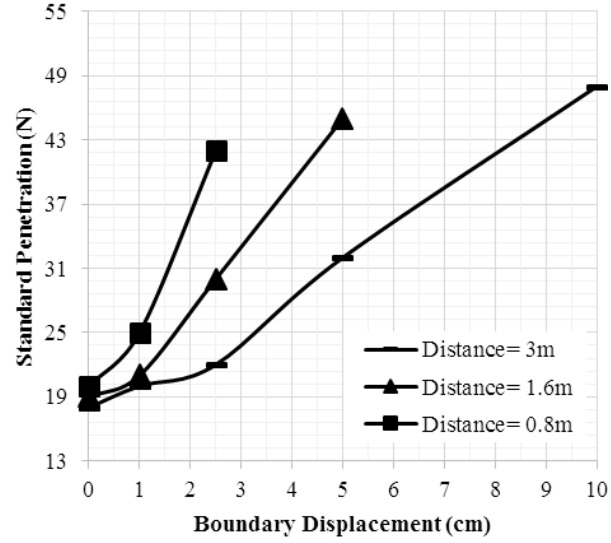


Figure 11. Comparison of N_{SPT} changes with boundary displacement at the depth of 12m.

[Downloaded from ndea10.khu.ac.ir on 2026-11-02]

[DOR: 20.1001.1.22286837.1398.13.5.2.1]

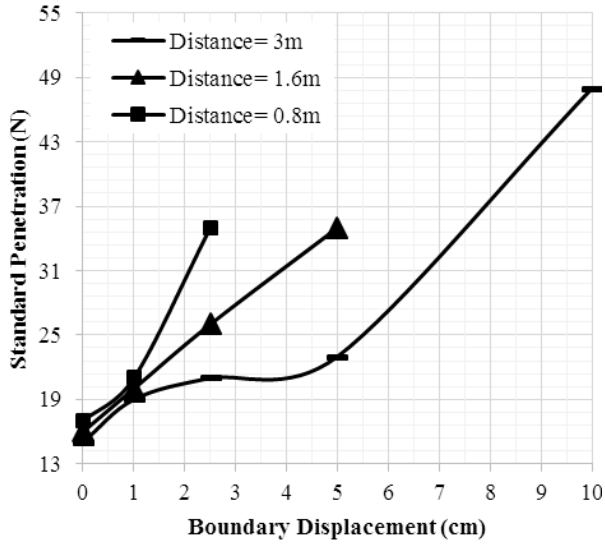


Figure 12. Comparison of N_{SPT} changes with boundary displacement at the depth of 13.5m.

So, it is advised to apply different injection pressure for each depth separately as a multipurpose: 1) modification of liquefiable soil by sufficient injection pressure, 2) Not causing failure by overpressure of injection. It was observed the most liquefiable layer between 12 to 16 meters. So, it could be achieved safe area by increasing the boundary displacement to make the soil layer denser. The normalized curves of safety factor of loose silty sand, due to micropile installation are reported as Figure 15, for 3m spacing of micropiles.

It can be concluded that the normalized safety factors above 2 are representative trusted zone against liquefaction. The closer distances of micropiles have so $N_{(SPT)}$ and consequently so safety factor that it is not available any quantitative data to show in the curves.

[Downloaded from ndea10.khu.ac.ir on 2026-11-02]

[DOR: 20.1001.1.22286837.1398.13.5.2.1]

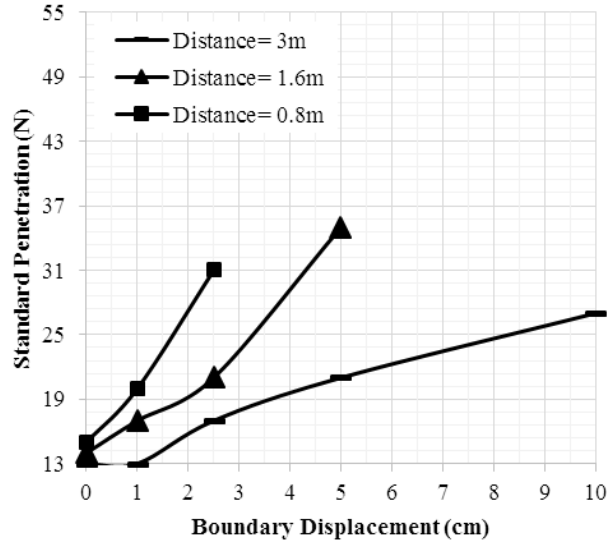


Figure 13. Comparison of N_{SPT} changes with boundary displacement at the depth of 15m.

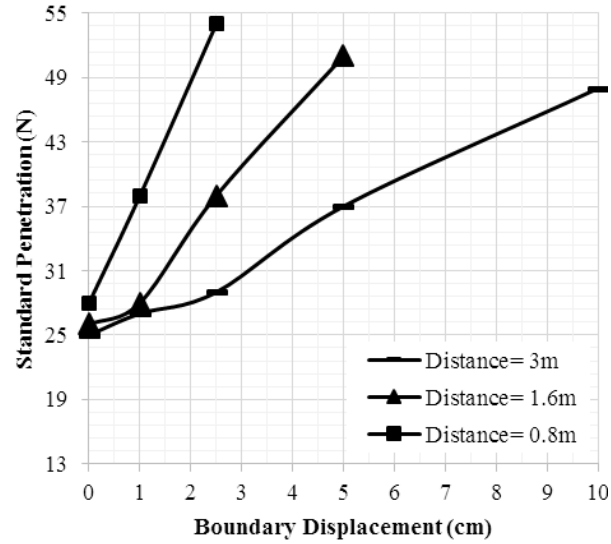


Figure 14. Comparison of N_{SPT} changes with boundary displacement at the depth of 17m.

[Downloaded from ndea10.khu.ac.ir on 2026-11-02]

[DOR: 20.1001.1.22286837.1398.13.5.2.1]

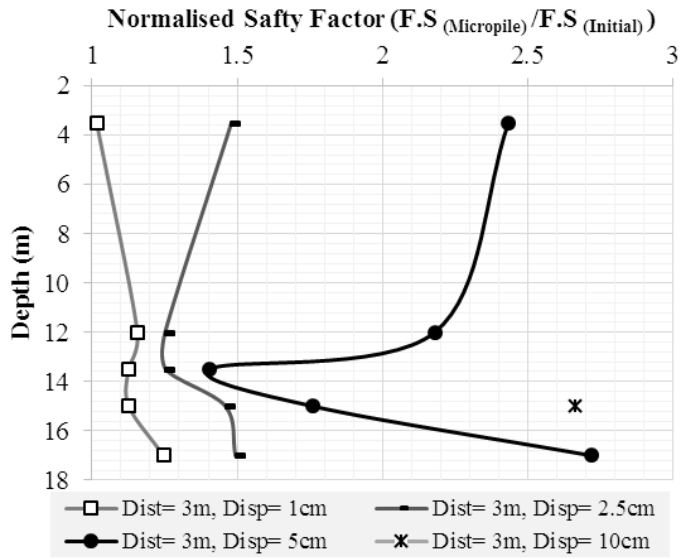


Figure 15. Comparison of normalized safety factor changes with depth at 3m distances of micropiles and 4 boundary displacement.

Figure 15 shows the amount of modification rather than the base situation without any micropile installation at 3m distances of micropiles. So, the best results achieved from 2.5 to 5 cm boundary displacement. The soil layer presents more modification by accepting 1cm boundary displacement at 12m micropile depth rather than 3.5m micropile depth. It shows that low injection pressure causes eligible modification at the soil layers with low confinement; although there is another factor (micropile distances) to change the pattern of soil improvement. Also, it is concluded that the increase in injection pressure up to an optimum amount is desirable, but higher amounts cannot be efficient; so it seems to be better to use various pressure for every depth.

[Downloaded from ndea10.khu.ac.ir on 2026-11-02]

[DOR: 20.1001.1.22286837.1398.13.5.2.1]

Table 4. Final results of indirect modeling in estimating liquefaction potential on the basis of borehole specifications

Micropiles distances (m)														
3						1.6				0.8				
Boundary displacement representative injection pressure														
CSR	10 cm	5 cm	2.5 cm	1 cm	0	5 cm	2.5 cm	1 cm	0	2.5 cm	1 cm	0		Depth (m)
0.468	≥40	35	27	22	21	49	35	25	22	≥40	30	23	N60	3.5
		0.567	0.345	0.237	0.228		0.567	0.293	0.234		0.391	0.254	CRR	
		1.212	0.737	0.506	0.498		1.21	0.626	0.50		0.83	0.541	F.S.	
0.411	48	32	22	20	18	45	30	21	19	42	25	20	N60	12
		0.413	0.237	0.219	0.189		0.391	0.228	0.201		0.293	0.219	CRR	
		1.005	0.577	0.533	0.46		1.33	0.555	0.489		0.713	0.531	F.S.	
0.398	48	23	21	19	15	35	26	20	16	35	21	17	N60	13.5
		0.254	0.228	0.204	0.17	0.567	0.313	0.219	0.177	0.567	0.228	0.18	CRR	
		0.64	0.572	0.513	0.456	1.424	0.786	0.55	0.445	1.424	0.573	0.452	F.S.	
0.365	27	21	17	13	13	35	21	17	14	31	20	15	N60	15
	0.345	0.228	0.189	0.146	0.146	0.567	0.228	0.189	0.159	0.402	0.219	0.17	CRR	
	0.945	0.625	0.518	0.4	0.355	1.55	0.625	0.518	0.436	1.101	0.6	0.466	F.S.	
0.334	48	37	29	27	25	51	38	28	26	54	37	28	N60	17
		0.742	0.407	0.34	0.293		0.846	0.367	0.313		0.742	0.367	CRR	
		2.222	1.22	1.018	0.698		2.53	1.099	0.937		2.22	1.099	F.S.	

Conclusions

Two kinds of simulation were run to estimate the liquefaction potential of saturated sand. So the results can be declared as following, separately.

Generally, simulation of standard penetration test in the mentioned software as direct modeling is not preferable because some points were not considered such as the effect of rod penetration

[Downloaded from ndea10.khu.ac.ir on 2026-11-02]

[DOR: 20.1001.1.22286837.1398.13.5.2.1]

and subsequently the rod-soil friction, cross section of rod tip, change in stress level after every hammer fall and then change in compression and mechanical specification of soil layer. In direct modeling, for shallow depths, the results of SPT simulation are consistent with real results by using Mohr-Columb constitutive model. Also, by increasing the depth of the test, PLAXIS shows fewer amounts than real results of N_{SPT}. It could be better to use hardening soil model to decreases the error of inequality. So, simulation of SPT may help to estimate the effect of micropile installation by measuring N_{SPT}.

In indirect modeling, the effect of injection pressure on $N_{(SPT)}$ at either constant distance or constant depth were studied. It was concluded that by increasing injection pressure (boundary displacement), more modification is achieved. Because the software is not sentient, it is required a geotechnics professional to eliminate the wrong data such as relative density higher than 1. For closer micropiles, modification is estimated by less grouting and less injection pressure. So, the favorable safety factor was attained at lower injection pressure. If the boundary displacements were supposed to be the maximum penetration of slurry, there is a compatibility between results of indirect modeling and FHWA criteria which introduces 1.5D (D is diameter of borehole) as the maximum grout penetration. In situ injection pressure (1.2 MPa) at 3m distance of micropiles is equal to 5 to 10 cm boundary displacement (1.5D to 2D). This shows that higher injection

[Downloaded from ndea10.khu.ac.ir on 2026-11-02]

[DOR: 20.1001.1.22286837.1398.13.5.2.1]

pressures up to 8 MPa are used for unsaturated or drained soils. By the way, there would be likely under scour and dilution of slurry in saturated soils. The results of the models are less than site observations. So, the software eventuates some conservative data. The maximum error of this kind of simulation is low. Finally, it can be concluded that indirect modeling with every applied simplifications and its special philosophy, would comprise some acceptable results.

References

1. Juran I., Bruce D. A., Dimillio A., Benslimane A., "Micropiles: The state of practice. Part II: Design of single micropiles and groups and networks of micropiles", Journal of Ground Improvement, No. 3 (1999).
2. Bruce D. A., Cadden A. W., Sabatini P. J., "Practical Advice for Foundation Design-Micropiles for Structural Support", contemporary issues in foundation engineering (2004).
3. Misra A., Chen C. H., Oberoi R., Klwiber A., "Simplified analysis method for micropile pullout behavior", Journal of Geotechnical and Geoenvironmental Engineering, Vol. 130, No. 10 (2004) 1024-1033.
4. Misra A., Roberts l. A, Oberoi R, and Chen C. H., "Uncertainty analysis of micropile pullout based upon load test results", Journal of Geotechnical and Geo-Environmental Engineering, Vol. 133, No. 8, (2007) 1017-1025.
5. Russo G., "Full-scale load tests on instrumented micropiles", Geotechnical Engineering Journal, Vol. 157. No.3 (2004) 127-135.
6. Han J., and Ye S.L., "A field study on the behavior of micropiles in clay under compression or tension", Canadian Geotechnical Journal, 43,19-29, (2006).

[Downloaded from ndea10.khu.ac.ir on 2026-11-02]

[DOR: 20.1001.1.22286837.1398.13.5.2.1]

7. Korolev V. M., Argal E. S., "Investigation of the stress state of micropiles", Soil Mechanics and Foundation Engineering. Vol. 45, No. 5 (2008) 9-12.
8. Sharma B., Zaheer S., Hussain Z., "Experimental Model for Studying the Performance of Vertical and Batter Micropiles", Geo-Congress 2014 Technical Papers (2014) 4252-4264.
9. Sharma B., Hussain Z., "A Model Study of Micropile Groups Subjected to Lateral Loading Condition", Proceedings of Indian Geotechnical Conference (2011).
10. Veludo J., Julio E. N. B. S., Dias-da-Costa D., "Compressive strength of micropile-to-grout connections", Construction and Building Materials. 26 (2012) 172-179.
11. Galli A., di Prisco C., "Displacement-based design procedure for slope-stabilizing piles", Can. Geotech. J. 50 (2013) 41-53.
12. Muthukkumaran K., "Effect of Slope and Loading Direction on Laterally Loaded Piles in Cohesionless Soil", International Journal of Geomechanics (2013).
13. Ousta R., Shahrour I., "Three-dimentional analysis of the seismic behavior of micropiles used in the reinforcement of saturated soil", International Journal for Numerical and Analytical Methods in Geomechanics." Vol. 25, No. 2 (2001) 183-196.
14. Shahrour I., Sadek M., "Three-dimensional finite element analysis of the seismic behavior of inclined micropiles", Soil Dynamics and Earthquake Engineering. 24 (2004) 473-485.
15. Shahrour I., Sadek M., "Influence of the head and tip connection on the seismic performance of micropiles", Soil Dynamics and Earthquake Engineering, 26 (2006) 461-468.

[Downloaded from ndea10.khu.ac.ir on 2026-11-02]

[DOR: 20.1001.1.22286837.1398.13.5.2.1]

16. Alsaleh H., Shahrour I., "Influence of plasticity on the seismic soil-micropiles-structure interaction", International Journal of Soil Dynamics and Earthquake Engineering. Vol. 29, No. 3 (2009) 574-578.
17. Ghorbani A., et al., "Comprehensive three dimensional finite element analysis, parametric study and sensitivity analysis on the seismic performance of soil–micropile-superstructure interaction", Soil Dynamics and Earthquake Engineering. Volume 58, March 2014, Pages (2014) 21-36.
18. Babu G. L., Murthy B., Nataraj M. S., "Bearing capacity improvement using micropiles: A case study", Proceedings, Geosupport Conference (2004) 692-699.
19. McManus K. J., Charton G., Turner J. P., "Effect of micropiles on seismic shear strain", Proceeding, Geo Support Conf. ASCE. New York, (2004).
20. Sabatini P. J., "Micropile design and construction." Report No. FHWA-NHI-05-039 (2005).
21. Teunissen J. A. M., "Fracture calculations (In Dutch)", GeoDelft internal technical note (2006) 14-02.
22. Hassanlourad M., Sarrafi A., "Investigation of Sandy Soils Grout-ability with Sodium Silicate Chemically Grout", Amirkabir Journal of science and technology (2014).
23. Ribeiri D., Cardoso R., "A review on models for the prediction of the diameter of jet grouting columns", European Journal of Environmental and Civil Engineering (2016).
24. Wang Z. F., Bian X and Wang Y. Q., "Numerical approach to predict ground displacement caused by installing a horizontal jet grout column", Marine Geosources & Geotechnology (2016).

[Downloaded from ndea10.khu.ac.ir on 2026-11-02]

[DOR: 20.1001.1.22286837.1398.13.5.2.1]

25. Shen S. L., Wang Z. F., Cheng W. C., "Estimation of lateral displacement induced by jet grouting in clayey soils", Géotechnique (2017).
26. Sarker D., ZoynulAbedin M. D., "MATLAB Modeling of SPT and Grain Size Data in Producing Soil-Profile", International Journal of Science and Engineering Investigations (2015).
27. Anwar A., Jamal Y., Ahmad S., Khan M. Z., "Assessment of Liquefaction Potential of Soil Using Multi-linear Regression Modeling", International Journal of Civil Engineering and Technology (IJCIET), (2016).
28. Kumar R., Bhargava K., Choudhury D., "Estimation of Engineering Properties of Soils from Field SPT Using Random Number Generation", Indian National Academy of Engineering (2016).
29. Prasad H. D., Puri N. Jain A., "Prediction of In-Place Density of Soil Using SPT N-Value", Conference on Numerical Modeling in Geomechanics (CoNMiG-2017) (2017).
30. GuhaRay A., Mohammed Y., Harisankar S. and Gowre M. S., "Effect of micropiles on liquefaction of cohesionless soil using shake table tests", Innovation of Infrastructure Solutions (2017).
31. Naeini S. A. and Hamidzadeh M., "Using Micropiles to Improve the Anzali's Saturated Loose Silty Sand", International Journal of Environmental, Chemical, Ecological, Geological and Geophysical Engineering (2017).
32. ZiaeiMoayed S. R., Naeini S. A., "Improvement of Loose Sandy Soil Deposits using Micropiles", KSCE Journal of Civil Engineering. 16 (3) (2012) 334-340.
33. Bowles J. E., "Foundation Analysis and Design (5^{th}edn)", Peoria. Illinois. The McGraw-Hill Companies, Inc (1997).

[Downloaded from ndea10.khu.ac.ir on 2026-11-02]

[DOR: 20.1001.1.22286837.1398.13.5.2.1]